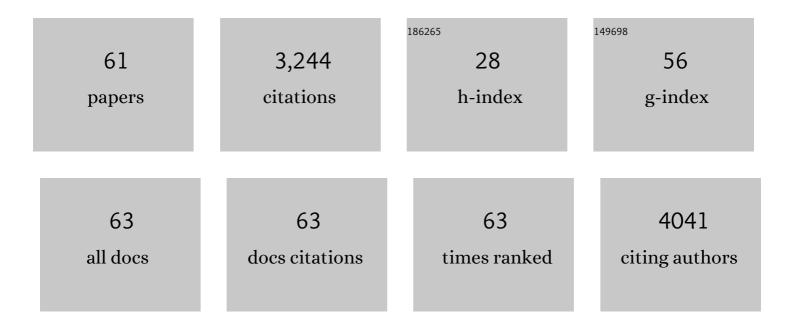
## Jianbing Zhang

List of Publications by Year in descending order

Source: https://exaly.com/author-pdf/7488314/publications.pdf Version: 2024-02-01



LIANBING 7HANG

#	Article	IF	CITATIONS
1	Efficient and Reabsorptionâ€Free Radioluminescence in Cs <sub>3</sub> Cu <sub>2</sub> I <sub>5</sub> Nanocrystals with Selfâ€Trapped Excitons. Advanced Science, 2020, 7, 2000195.	11.2	282
2	Diffusion-Controlled Synthesis of PbS and PbSe Quantum Dots with <i>in Situ</i> Halide Passivation for Quantum Dot Solar Cells. ACS Nano, 2014, 8, 614-622.	14.6	256
3	PbSe Quantum Dot Solar Cells with More than 6% Efficiency Fabricated in Ambient Atmosphere. Nano Letters, 2014, 14, 6010-6015.	9.1	212
4	Metal Halide Solid-State Surface Treatment for High Efficiency PbS and PbSe QD Solar Cells. Scientific Reports, 2015, 5, 9945.	3.3	205
5	Photophysics in Cs <sub>3</sub> Cu <sub>2</sub> X <sub>5</sub> (X = Cl, Br, or I): Highly Luminescent Self-Trapped Excitons from Local Structure Symmetrization. Chemistry of Materials, 2020, 32, 3462-3468.	6.7	177
6	Surface Passivation of Bismuth-Based Perovskite Variant Quantum Dots To Achieve Efficient Blue Emission. Nano Letters, 2018, 18, 6076-6083.	9.1	157
7	PbSe Quantum Dots Sensitized High-Mobility Bi <sub>2</sub> O <sub>2</sub> Se Nanosheets for High-Performance and Broadband Photodetection Beyond 2 μm. ACS Nano, 2019, 13, 9028-9037.	14.6	149
8	Revisiting the Valence and Conduction Band Size Dependence of PbS Quantum Dot Thin Films. ACS Nano, 2016, 10, 3302-3311.	14.6	118
9	Synthetic Conditions for High-Accuracy Size Control of PbS Quantum Dots. Journal of Physical Chemistry Letters, 2015, 6, 1830-1833.	4.6	109
10	Preparation of Cd/Pb Chalcogenide Heterostructured Janus Particles <i>via</i> Controllable Cation Exchange. ACS Nano, 2015, 9, 7151-7163.	14.6	97
11	Highly Luminescent Zero-Dimensional Organic Copper Halides for X-ray Scintillation. Journal of Physical Chemistry Letters, 2021, 12, 6919-6926.	4.6	95
12	Lead Selenide (PbSe) Colloidal Quantum Dot Solar Cells with >10% Efficiency. Advanced Materials, 2019, 31, e1900593.	21.0	80
13	Cationâ€Exchange Synthesis of Highly Monodisperse PbS Quantum Dots from ZnS Nanorods for Efficient Infrared Solar Cells. Advanced Functional Materials, 2020, 30, 1907379.	14.9	80
14	A New Passivation Route Leading to Over 8% Efficient PbSe Quantumâ€Đot Solar Cells via Direct Ion Exchange with Perovskite Nanocrystals. Advanced Materials, 2017, 29, 1703214.	21.0	69
15	Accelerated formation and improved performance of CH <sub>3</sub> NH <sub>3</sub> PbI <sub>3</sub> -based perovskite solar cells via solvent coordination and anti-solvent extraction. Journal of Materials Chemistry A, 2017, 5, 4190-4198.	10.3	65
16	Facet Control for Trap‧tate Suppression in Colloidal Quantum Dot Solids. Advanced Functional Materials, 2020, 30, 2000594.	14.9	60
17	Efficient Dual-Band White-Light Emission with High Color Rendering from Zero-Dimensional Organic Copper Iodide. ACS Applied Materials & Interfaces, 2021, 13, 22749-22756.	8.0	57
18	Significant Improvement in the Performance of PbSe Quantum Dot Solar Cell by Introducing a CsPbBr <sub>3</sub> Perovskite Colloidal Nanocrystal Back Layer. Advanced Energy Materials, 2017, 7, 1601773.	19.5	56

JIANBING ZHANG

#	Article	IF	CITATIONS
19	Controllable Synthesis of Two-Dimensional Ruddlesden–Popper-Type Perovskite Heterostructures. Journal of Physical Chemistry Letters, 2017, 8, 6211-6219.	4.6	54
20	Carrier Transport in PbS and PbSe QD Films Measured by Photoluminescence Quenching. Journal of Physical Chemistry C, 2014, 118, 16228-16235.	3.1	50
21	Controlled synthesis and photostability of blue emitting Cs <sub>3</sub> Bi <sub>2</sub> Br <sub>9</sub> perovskite nanocrystals by employing weak polar solvents at room temperature. Journal of Materials Chemistry C, 2019, 7, 3688-3695.	5.5	50
22	Solution-processed solar-blind deep ultraviolet photodetectors based on strongly quantum confined ZnS quantum dots. Journal of Materials Chemistry C, 2018, 6, 11266-11271.	5.5	46
23	Combination of Cation Exchange and Quantized Ostwald Ripening for Controlling Size Distribution of Lead Chalcogenide Quantum Dots. Chemistry of Materials, 2017, 29, 3615-3622.	6.7	44
24	Colloidal synthesis of lead-free all-inorganic cesium bismuth bromide perovskite nanoplatelets. CrystEngComm, 2018, 20, 7473-7478.	2.6	44
25	One-pot synthesis of hydrophilic CuInS <sub>2</sub> and CuInS <sub>2</sub> –ZnS colloidal quantum dots. Journal of Materials Chemistry C, 2014, 2, 4812-4817.	5.5	43
26	Cu <sup>2+</sup> -Doped CsPbI <sub>3</sub> Nanocrystals with Enhanced Stability for Light-Emitting Diodes. Journal of Physical Chemistry Letters, 2021, 12, 3038-3045.	4.6	37
27	Realizing Near-Unity Quantum Efficiency of Zero-Dimensional Antimony Halides through Metal Halide Structural Modulation. ACS Applied Materials & Interfaces, 2021, 13, 58908-58915.	8.0	36
28	Ligand-Engineered HgTe Colloidal Quantum Dot Solids for Infrared Photodetectors. Nano Letters, 2022, 22, 3465-3472.	9.1	36
29	Efficiently Passivated PbSe Quantum Dot Solids for Infrared Photovoltaics. ACS Nano, 2021, 15, 3376-3386.	14.6	32
30	In Situ Tuning the Reactivity of Selenium Precursor To Synthesize Wide Range Size, Ultralarge-Scale, and Ultrastable PbSe Quantum Dots. Chemistry of Materials, 2018, 30, 982-989.	6.7	27
31	Enhanced Passivation and Carrier Collection in Ink-Processed PbS Quantum Dot Solar Cells via a Supplementary Ligand Strategy. ACS Applied Materials & Interfaces, 2020, 12, 42217-42225.	8.0	27
32	Hybrid Growth Modes of PbSe Nanocrystals with Oriented Attachment and Grain Boundary Migration. Advanced Science, 2019, 6, 1802202.	11.2	26
33	Quantum Confinement-Tunable Ultrafast Charge Transfer in a PbS Quantum Dots/WSe <sub>2</sub> 0D–2D Hybrid Structure: Transition from the Weak to Strong Coupling Regime. Journal of Physical Chemistry Letters, 2019, 10, 7665-7671.	4.6	25
34	Low cost and large scale synthesis of PbS quantum dots with hybrid surface passivation. CrystEngComm, 2017, 19, 946-951.	2.6	24
35	Enhanced Photoluminescence of Colloidal Leadâ€Free Double Perovskite Cs <sub>2</sub> Ag <sub>1â^²</sub> <i><sub>x</sub></i> Na <i><sub>x</sub></i> Na <i>Sub&gt;x</i> Na <i><sub>x</sub></i> Na <i><sub>x</sub></i>	7.3	24
36	Phosphine-free synthesis and shape evolution of MoSe <sub>2</sub> nanoflowers for electrocatalytic hydrogen evolution reactions. CrystEngComm, 2018, 20, 2491-2498.	2.6	21

JIANBING ZHANG

#	Article	IF	CITATIONS
37	Efficient PbSe Colloidal Quantum Dot Solar Cells Using SnO <sub>2</sub> as a Buffer Layer. ACS Applied Materials & Interfaces, 2020, 12, 2566-2571.	8.0	21
38	Highly Luminescent Zero-Dimensional Organic Copper Halide with Low-Loss Optical Waveguides and Highly Polarized Emission. , 2022, 4, 1446-1452.		21
39	Improving carrier extraction in a PbSe quantum dot solar cell by introducing a solution-processed antimony-doped SnO <sub>2</sub> buffer layer. Journal of Materials Chemistry C, 2018, 6, 9861-9866.	5.5	20
40	Matching Charge Extraction Contact for Infrared PbS Colloidal Quantum Dot Solar Cells. Small, 2022, 18, e2105495.	10.0	20
41	Singleâ€Component Whiteâ€Light Emitters with Excellent Color Rendering Indexes and High Photoluminescence Quantum Efficiencies. Advanced Optical Materials, 2022, 10, .	7.3	18
42	Highly luminescent zero-dimensional lead-free manganese halides for Î <sup>2</sup> -ray scintillation. Nano Research, 2022, 15, 8486-8492.	10.4	18
43	Self-assembly and photoactivation of blue luminescent CsPbBr <sub>3</sub> mesocrystals synthesized at ambient temperature. Journal of Materials Chemistry C, 2018, 6, 1701-1708.	5.5	17
44	Efficient Infrared Solar Cells Employing Quantum Dot Solids with Strong Interâ€Đot Coupling and Efficient Passivation. Advanced Functional Materials, 2021, 31, 2006864.	14.9	16
45	Carrier Transport Dynamics in High Speed Black Phosphorus Photodetectors. ACS Photonics, 2018, 5, 1412-1417.	6.6	15
46	Nonvolatile Resistive Switching Memory Device Employing CdSe/CdS Core/Shell Quantum Dots as an Electrode Modification Layer. ACS Applied Electronic Materials, 2020, 2, 827-837.	4.3	15
47	Sublimation and related thermal stability of PbSe nanocrystals with effective size control evidenced by in situ transmission electron microscopy. Nano Energy, 2020, 75, 104816.	16.0	13
48	Bright infra-red quantum dot light-emitting diodes through efficient suppressing of electrons. Applied Physics Letters, 2020, 116, .	3.3	11
49	In-situ observation of trapped carriers in organic metal halide perovskite films with ultra-fast temporal and ultra-high energetic resolutions. Nature Communications, 2021, 12, 1636.	12.8	11
50	Temporal evolutions of the photoluminescence quantum yields of colloidal InP, InAs and their core/shell nanocrystals. Journal of Materials Chemistry C, 2014, 2, 4442-4448.	5.5	8
51	Sub-50 picosecond to microsecond carrier transport dynamics in pentacene thin films. Applied Physics Letters, 2018, 113, 183509.	3.3	8
52	Manipulating Charge Transfer from Core to Shell in CdSe/CdS/Au Heterojunction Quantum Dots. ACS Applied Materials & Interfaces, 2019, 11, 48551-48555.	8.0	7
53	Controlled synthesis of brightly fluorescent CH <sub>3</sub> NH <sub>3</sub> PbBr <sub>3</sub> perovskite nanocrystals employing Pb(C <sub>17</sub> H <sub>33</sub> COO) <sub>2</sub> as the sole lead source. RSC Advances, 2018, 8, 1132-1139.	3.6	6
54	Triplet energy migration pathways from PbS quantum dots to surface-anchored polyacenes controlled by charge transfer. Nanoscale, 2021, 13, 1303-1310.	5.6	5

JIANBING ZHANG

#	Article	IF	CITATIONS
55	CsPb(Br/Cl)3 Perovskite Nanocrystals with Bright Blue Emission Synergistically Modified by Calcium Halide and Ammonium Ion. Nanomaterials, 2022, 12, 2026.	4.1	5
56	Synthesis of Highly Luminescent InP/ZnS Quantum Dots with Suppressed Thermal Quenching. Coatings, 2021, 11, 581.	2.6	4
57	Efficient Enhancement of Stability and Luminescence of Three-Dimensional CsPbBr <sub>3</sub> Nanoparticles via Ligand-Triggered Transformation into Zero-Dimensional Cs <sub>4</sub> PbBr <sub>6</sub> Nanoparticles. Journal of Physical Chemistry C, 2022, 126, 4172-4181.	3.1	4
58	Phosphine-free synthesis and optical stabilities of composition-tuneable monodisperse ternary PbSe <sub>1â^x</sub> S <sub>x</sub> alloyed nanocrystals <i>via</i> cation exchange. CrystEngComm, 2018, 20, 2519-2527.	2.6	3
59	Highly sensitive SWIR photodetector using carbon nanotube thin film transistor gated by quantum dots heterojunction. Applied Physics Letters, 2022, 120, .	3.3	3
60	Generating and Capturing Secondary Hot Carriers in Monolayer Tungsten Dichalcogenides. Journal of Physical Chemistry Letters, 2022, 13, 5703-5710.	4.6	2
61	Electron Beam Induced Formation of Hollow RbBr Nanocubes. Journal of Physical Chemistry C, 2018, 122, 28347-28350.	3.1	0